Species-area relationships and extinctions caused by habitat loss and fragmentation: Supplementary information[†]

Joel Rybicki[1] and Ilkka Hanski[*2]

[1]Department of Computer Science, University of Helsinki
[2]Department of Biosciences, University of Helsinki

S1 The stochastic patch occupancy model

The metapopulation dynamics of the species are modelled as a discrete-time, spatially explicit stochastic patch occupancy model (SPOM). The community consists of species with distinct ecological traits, but there are no interactions between the species.

The landscape. The network of habitat patches consists of a finite two-dimensional grid with dimensions $N_0 \times N_1$. Each cell in the grid corresponds to a patch which may be occupied by local populations of the species. We will identify each patch in the network with its co-ordinates $\mathbf{u} = (u_0, u_1)$, where $u_0 \in \{0, 1, \ldots, N_0 - 1\}$ and $u_1 \in \{0, 1, \ldots, N_1 - 1\}$. It is natural to define the distance between two patches $\mathbf{u}$ and $\mathbf{v}$ as

$$d(\mathbf{u}, \mathbf{v}) = \sqrt{(u_0 - v_0)^2 + (u_1 - v_1)^2}, \tag{1}$$

which is the two-dimensional Euclidean distance between the points. The habitat type of each patch $\mathbf{u}$ is described by a real value $H(\mathbf{u}) \in [0, 1]$. The habitat type of patches are spatially correlated (see below).

Species parameters. Each species is characterised by a tuple $\mathbf{s} = (\alpha, c, e, \varphi, \gamma)$ of five parameters. The value $\alpha^{-1} \in \mathbb{R}^+$ is the average dispersal distance of the species, where α is the parameter of the exponential dispersal kernel

$$f(r) = \frac{\alpha^2}{2\pi} \exp(-r\alpha). \tag{2}$$

The value $f(r)$ is the fraction of propagules reaching distance r from a given point. The normalisation factor $\alpha^2/2\pi$ ensures that

$$\int_{\mathbf{x} \in \mathbb{R}^2} f(d(\mathbf{0}, \mathbf{x})) = \int_0^\infty 2\pi r f(r) \, \mathrm{d}r = 1.$$

Since we run our simulation on a finite grid, this essentially means that no propagules arrive from outside the network, while some propagules may leave the network particulary near the edges of the grid.

[†]Revised version, January 2014.
[*]Corresponding author. E-mail: ilkka.hanski@helsinki.fi

The colonization and extinction rates of the species are determined by the positive real values c and e, respectively. The parameter $\varphi \in [0, 1]$ describes the phenotype of the species which, together with habitat type, determines the fitness of the species. Given habitat type h, the fitness of the species is determined by the Gaussian function

$$g(h) = \exp\Big(-\frac{(h-\varphi)^2}{2\gamma^2}\Big), \tag{3}$$

where γ is a positive real parameter called niche width. The niche width controls the width of the bell in the Gaussian curve. Thus, generalist species have a large γ and specialist species have small γ.

Dynamics. The metapopulation dynamics are modeled as a discrete-time Markov chain. The state of the system at each time step $t \in \{0, 1, 2, \dots\}$ is given by the patch occupancy matrices of all the species. Since each species is independent in our model, that is, there are no interactions between the species, and to avoid unnecessarily complex notation, we describe the dynamics for a single species.

The occupancy state of each patch $\mathbf{u}$ at time t is binary value denoted by $O(\mathbf{u}, t) \in \{0, 1\}$. The patch $\mathbf{u}$ is occupied at time t if and only if $O(\mathbf{u}, t) = 1$. The state transition probabilities depend on the colonization and extinction rates of the species and on the quality and connectivity of the patch.

We define the quality of the patch as a function of the habitat type and the fitness function g of the species:

$$q(\mathbf{u}) = g(H(\mathbf{u})). \tag{4}$$

The connectivity of a patch is determined by the dispersal ability of the species and the quality of the patch. Consider a patch $\mathbf{u}$ at the time step t. Formally, the connectivity of a patch is defined as the sum

$$S(\mathbf{u}, t) = \sum_{\mathbf{v} \neq \mathbf{u}} O(\mathbf{v}, t) q(\mathbf{v}) f\big(d(\mathbf{u}, \mathbf{v})\big). \tag{5}$$

Note that only occupied patches contribute to connectivity. In previous work, the areas of patches have often been assumed to influence the contribution of a source patch to the connectivity of a target patch (Ovaskainen & Hanski 2004). In our model all patches are of the same size, but instead the quality of the patch (for a particular species) affects the connectivity.

For each patch there are two state transition probabilities depending on whether the patch is occupied or unoccupied. The probability that an unoccupied patch will be colonized is

$$\Pr[\mathbf{u} \text{ is occupied at step } t+1] = 1 - \exp(-cS(\mathbf{u}, t)), \tag{6}$$

and the extinction probability of a population in a patch is

$$\Pr[\mathbf{u} \text{ is unoccupied at step } t+1] = 1 - \exp\Big(-\frac{e}{q(\mathbf{u})}\Big). \tag{7}$$

Fast computation of connectivity. Given a grid consisting of n patches, computing the connectivity for all patches by directly using Equation 5 requires $\mathcal{O}(n^2)$ arithmetic operations. However, connectivity can be computed significantly faster by expressing it as a discrete two-dimensional convolution (Brewster & Allen 1997). Given two finite functions g and h, the discrete convolution $g \star h$ is defined as

$$(g \star h)(x) = \sum_y g(x - y) h(y). \tag{8}$$

For the sake of concise presentation, suppose the landscape is a square grid of size $N \times N$. Let $[N]^2$ denote the set of coordinates in the grid. We define two $2N \times 2N$ matrices A and K, where matrix A is given by

$$A(i,j) = \begin{cases} O(i,j,t)q(i,j) & \text{if } (i,j) \in [N]^2, \\ 0 & \text{otherwise.} \end{cases} \tag{9}$$

The matrix K is defined by $K(i,j) = f\big(\sqrt{\phi(i)^2 + \phi(j)^2}\big)$, where $\phi(i) = \min\{i, 2N - i\}$. It can be shown that for all $\mathbf{u} \in [N]^2$, the equality

$$(A \star K)(\mathbf{u}) = \sum_{\mathbf{v} \in [N]^2} O(\mathbf{u}, t)q(\mathbf{u})f\big(d(\mathbf{u}, \mathbf{v})\big) = S(\mathbf{u}, t) \tag{10}$$

holds. The convolution theorem states that $A \star K = \mathcal{F}^{-1}[\mathcal{F}(A) \cdot \mathcal{F}(K)]$, where $\mathcal{F}$ is the Fourier transform operator and $\cdot$ is the point-wise product of matrices. As the FFT algorithm can compute the discrete Fourier transform and its inverse in $\mathcal{O}(n \log n)$ operations, we can also compute the connectivity for all n patches in the landscape in $\mathcal{O}(n \log n)$ time.

S2 Generating habitat and regional stochasticity

This section describes the algorithms for generating the habitat types and regional stochasticity in the simulation software.

Spatially autocorrelated habitat type. The algorithm for generating a habitat matrix H with spatial variation is similar to the algorithm presented by Gu *et al.* (2002) for creating regional stochasticity. To control the scale of spatial autocorrelation, the algorithm takes a single parameter, $\omega > 0$, as input. The larger ω is, the greater the scale of spatial autocorrelation.

The algorithm is based on a recursive quadtree subdivision: recursively divide the grid into four rectangles down to single cells. To simplify the presentation, assume the landscape is a square of size $2^d \times 2^d$ for some positive integer d. Thus, the recursion will always proceed for d steps.

Consider the recursion at level $k \in \{1, \ldots, d\}$. Each rectangle generated during the previous step is divided into four subrectangles. Thus, at the kth recursion level, 4^k new rectangles will be created; we denote these rectangles as $A_{k,1}, \ldots, A_{k,4^k}$. For each rectangle $A_{k,\ell}$ we pick $X_{k,\ell}$ uniformly at random from the unit range $[0, 1]$. Let $w_k = \omega^{-k}$ be the weight of the level. Now the value of $H(i,j)$ is

$$H(i,j) = \frac{1}{W} \sum_{k=1}^{d} \sum_{\ell=1}^{4^k} [(i,j) \in A_{k,\ell}] w_k X_{k,\ell}, \tag{11}$$

where $W = \sum_{k=1}^{d} w_k$ is used to normalize the values into the unit range $[0, 1]$.

It is possible to use other schemes for setting the weights w_k, e.g., hand-picked values. However, using the parameter ω to define the weights is simple yet flexible enough for our purposes. In this work, we only consider cases where $\omega \in \{0.5, 1.0, 1.5, 2.0\}$ to get four different types of spatial autocorrelation. Figure S1 illustrates the types of landscapes generated by the algorithm.

We included an option to randomly shift the origo of the habitat matrix at each recursion depth k in order to vary the location of the borders of the different habitat types. This can be used to ensure that the changes in habitat type do not coincide with the sampling scheme for species-area relationships (see Section S3).

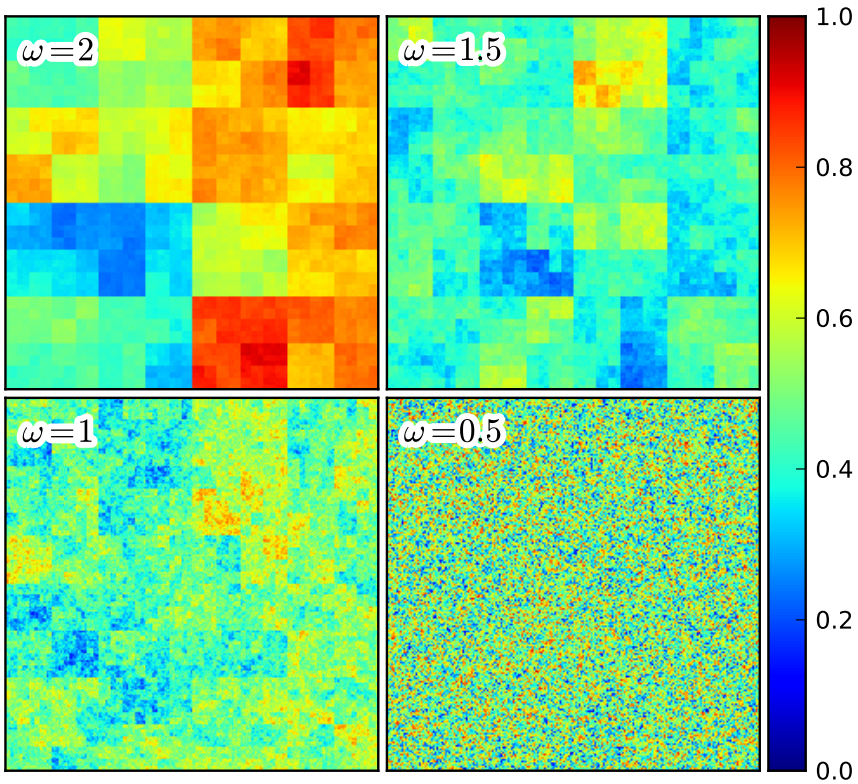

Figure S1: Randomly generated landscapes of size 512×512 with four different values of the parameter ω without origo shifting. The colours indicate habitat types of individual cells.

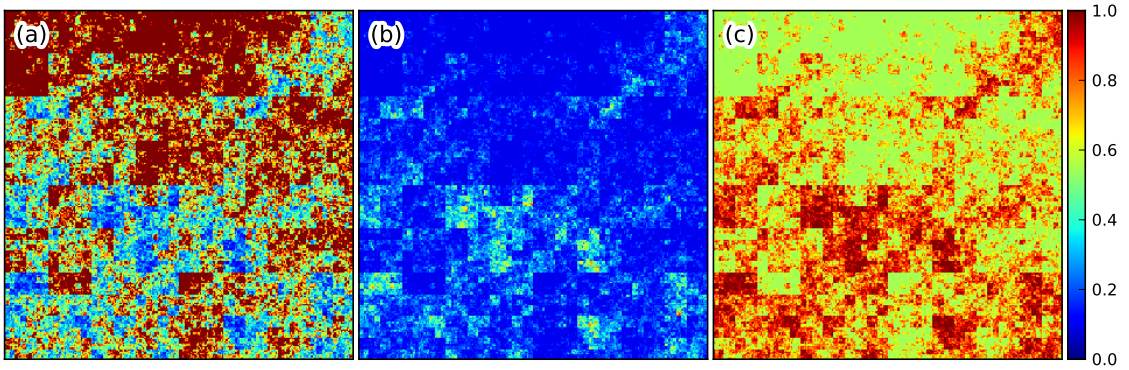

Figure S2: The effect of regional stochasticity on extinction probabilities. (a) Matrix E specifying regional stochasticity with $\mu = 0$, $\sigma = 0.75$ and $\omega = 1$. The colours of the pixels indicate the values affecting habitat quality. In dark red cells the habitat quality remains unaltered, whereas in blue cells the habitat quality is greatly reduced. (b) Extinction probabilities derived from matrix E for a species with extinction rate $e = 0.1$ in a landscape which all cells have habitat type φ (optimal habitat for the species). Here, the pixel colours indicate the extinction probability in a particular cell. Regional stochasticity may significantly increase the probability of extinction. (c) Extinction probabilities for a species with extinction rate $e = 0.1$ and niche width $\gamma = 0.1$ in a lanscape in which all cells have a slightly suboptimal habitat type, such that $|\varphi - h| = 0.05$.

Regional stochasticity. To model temporal variation in the environment, we generate a regional stochasticity matrix E. The matrix E is generated in a similar fashion as the spatially correlated habitat matrix with some minor differences.

First, we generate matrix E' as follows. Instead of choosing the random values from a uniform distribution, we use a normal distribution with mean $\mu = 0$ and variance σ^2. Second, the weights w_k are defined as above, but the normalization factor is

$$W' = \sqrt{\sum w_k^2}. \tag{12}$$

Now, each generated value $E'(i,j) = \sum a_k X_k$ is a linear combination of normally distributed variables, and hence also normally distributed. Dividing the values with the normalization factor W' yields a normally distributed value with $\mu = 0$ and variance σ^2. Finally, we define the value $E(i,j)$ as

$$E(i,j) = \max\{1, \exp\big(E(i,j)\big)\}, \tag{13}$$

which corresponds to a truncated log-normal distribution with $\mu = 0$ and variance σ^2. To incorporate regional stochasticity into the model, we modify the probability of extinction given in Equation (7) to

$$1 - \exp\Big(-\frac{e}{E(\mathbf{u})q(\mathbf{u})}\Big). \tag{14}$$

Figure S2 illustrates how regional stochasticity affects extinction probabilities.

Habitat fragmentation. We examine two different types of fragmentation patterns and their effects on species extinctions. The first pattern, maximal fragmentation, is created by choosing several disjoint areas for protection, while all habitat patches that are not

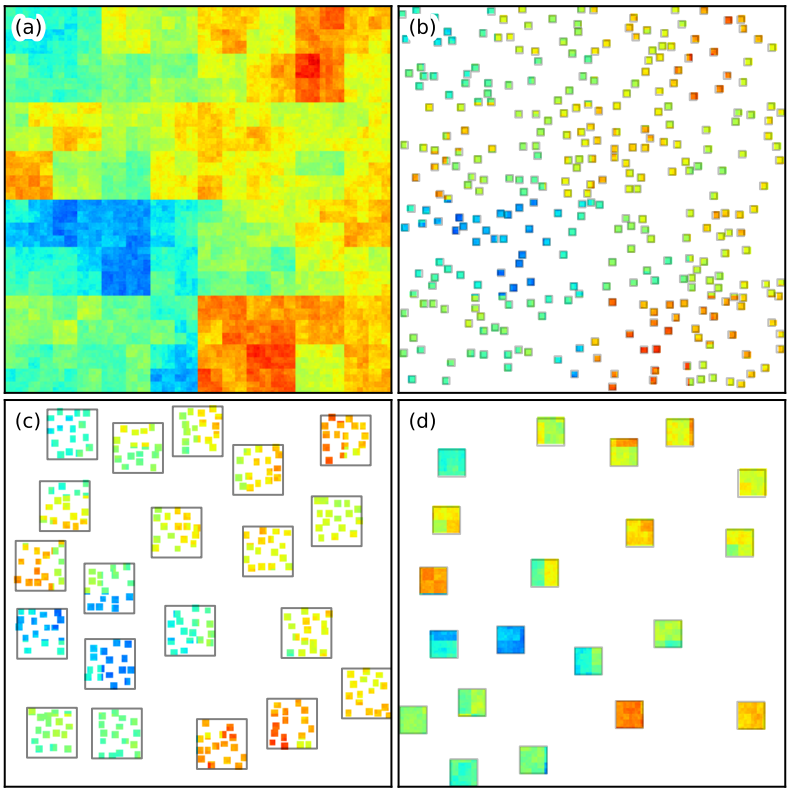

Figure S3: Fragmentation patterns with 10% habitat cover. (a) The original 512×512 landscape with $\omega = 1.5$. (b) Maximal fragmentation with 320 discrete fragments covering 10% of the habitat. (c) Clustered fragmentation with 20 clusters covering 33% of the landscape with each cluster containing 16 fragments that cover 30% of the cluster area. (d) Maximally fragmented landscape with 20 fragments that cover 10% of the total landscape.

contained in the selected areas are assigned negative habitat type indicating permanent habitat loss. In a patch with destroyed habitat, no dynamics besides extinction occur: all existing populations go extinct, and no new populations can colonize such a patch. Fragmentation is controlled by two parameters, the cover ratio $r \in [0, 1]$ and fragment number k. On a grid of size A, the algorithm randomly chooses k distinct fragments which cover approximately Ar patches in the landscape (grid cells).

The second pattern consists of clustered fragments. Instead of randomly choosing fragments throughout the landscape, we first choose k_C "cluster areas" with cover ratio r_C. Within each cluster area, we apply the first fragmentation pattern with parameters k_L and r_L. This gives a total of $Ar_C r_L$ grid cells located in $k_C k_L$ distinct fragments.

Using these two fragmentation patterns, we can create fragmented habitats with similar cover but clearly distinct spatial structure (Figure S3). For example, consider the following two cases. In the first case, apply the maximal fragmentation pattern with cover 0.1 and 100 fragments. For the second case, create clusters of fragments with parameters $c_C = \frac{1}{3}$, $c_L = \frac{3}{10}$, and $k_C = k_L = 10$. In both cases, the remaining habitat consists of 100 fragments each with area $\frac{A}{10^3}$. However, the cover ratio is locally much higher, as each cluster area in the clustered pattern has 30% of its area preserved as habitat. Figure S3 illustrates the two types of fragmentation patterns.

S3 Constructing species-area relationships

In this section, we describe how we construct SAR, RAR and OF-SARs.

SAR. We primarily consider the power-law SAR equation of the form

$$\frac{S_{\text{new}}}{S} = \Big(\frac{A_{\text{new}}}{A}\Big)^z, \tag{15}$$

where S_{new} is the average number of species contained within area A_{new}, A denotes the original habitat area and S is the number of non-extinct species in the area A. The equation can be easily derived from the conventional SAR with intercept $S_{\text{new}} = cA_{\text{new}}^z$ assuming the SAR slope remains constant at all spatial scales.

The SARs are constructed by sampling contiguous areas $A_0 \subset \cdots \subset A_k$ and recording the number S_i of the observed species in each area A_i. The landscape grid is divided into adjacent equally-sized squares each of which is used as a sampling area as shown in Figure S4. For each sample scale a_i, we count the average number of species in squares of size a_i. The resulting data points $\{(a_0, s_0), \ldots, (a_k, s_k)\}$ are fitted using linear regression to the log-log transformed SAR equation; see Section S4 for a brief discussion on other approaches for fitting SARs.

RAR. The remaining species-area relationship (RAR) is similar to SAR, but instead of counting the number of species occuring in the sample area, the number of endemic species is counted. RAR is given by the equation

$$\frac{S - S_{\text{loss}}}{S} = \Big(1 - \frac{a}{A}\Big)^z, \tag{16}$$

where S_{loss} is the average number of endemic species contained within area of size a. The data points given by $(S - S_{\text{loss}})/S$ and $(1 - a/A)$ are fitted to the log-log transformed RAR equation using linear regression.

One-fragment SARs. Here the landscape is divided into isolated habitat fragments of increasing size in the same manner as SAR sample areas are chosen. However, when

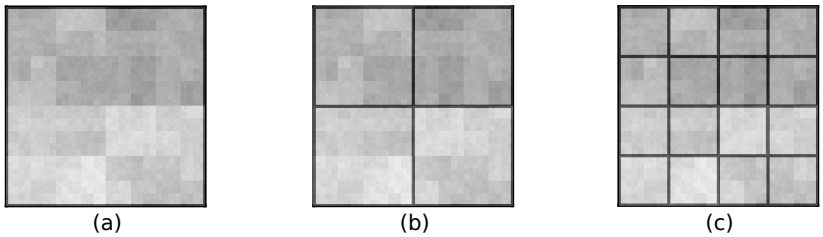

Figure S4: The recursive sampling scheme for SAR, RAR and OF-SAR. (a) The total number of species S is the number of non-extinct species in the entire landscape with area A. (b) The landscape is divided into four equally-sized squares with area $A/4$. By taking the average number of species occurring at each square, we get the average number of species in areas of size $A/4$. (c) Each square is again recursively divided into four smaller squares and the average number of species is computed by sampling each square as in the previous step. The process is repeated until the sample areas consist of single grid cells.

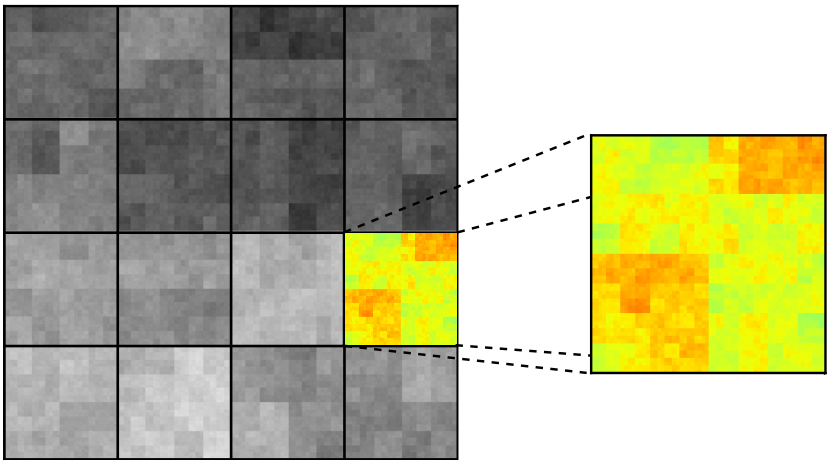

Figure S5: In OF-SAR, the landscape is divided into squares as in Figure S4 and each square is treated as an isolated habitat fragment. Each fragment is simulated in sequence for the same number of time steps. For all fragment sizes, we compute the average number of remaining species in fragments of the same size. The figure highlights an example of a single isolated habitat fragment of size 128×128 taken from a landscape with total area 512×512.

computing SAR, the simulation is first run for t steps on the entire landscape, whereas OF-SAR is computed by considering each sample area (fragment) as a separate landscape as illustrated in Figure S5. For each such fragment, the simulation is run for t rounds after which the number of non-extinct species is counted. Finally, we report the average number of species over all areas of the same size. The z-value for OF-SAR is computed by fitting the data to the log-log transformed SAR equation.

Constructing OF-SAR is computationally rather expensive compared to SAR and RAR, as a single simulation on a large landscape is not enough. Because each subarea is considered as an isolated landscape, the number of simulations (on the same set of species) grows exponentially with smaller sample areas: to compute the OF-SAR for a 512×512 landscape there are four 256×256 subareas, each with four 128×128 areas, and so on. In each of these, we simulate the same set of species separately.

S4 Simulation experiments

This section describes how the simulation experiments were conducted.

The effects of model parameters on species-area relationships. The effects of the model parameters on the RAR, SAR and OF-SAR were studied by running a simulation with an assemblage of 500 species on 512×512 landscapes. The species parameters were chosen uniformly at random from the ranges listed in Table S1.

After generating a random landscape and a random set of species with the specified parameters, the simulation was run for 500 time steps to ensure that most species would converge into their quasi-stationary states (metapopulation equilibria). The time to reach the quasi-stationary state depends on the habitat and species parameters, but we observed that for most species parameters a quasi-stationary state was reached well within 100 to 200 time steps. After the initial simulation, we computed SAR and RAR as described

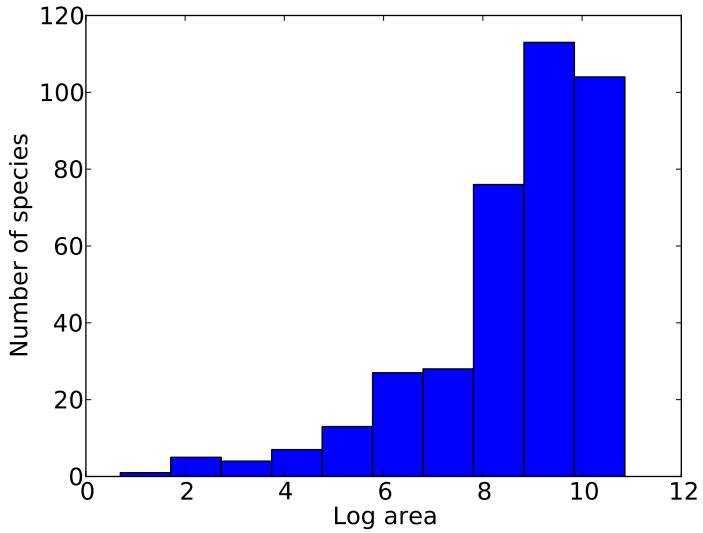

Figure S6: An example of the frequencies of the extent of species' distribution in quasi-stationary state. The x-axis gives the natural logarithm of the number of occupied cells and y-axis shows the number of species at each bin. The simulation parameters in this case are as follows. The habitat is a 512×512 grid with $\omega = 2$. Species parameters are $c \in (0.1, 0.15]$, $e \in (0.05, 0.1]$, $\alpha^{-1} \in \{1, 2, 3\}$ and $\varphi = 0.1$.

above. Similarly, OF-SAR was computed using the same habitat and the same set of species for 500 time steps on each isolated habitat fragment. Figure S6 gives an example of the extent of species' distributions in the quasi-stationary state.

To restrict the species-area relationships to the linear phase in log-log space, we omitted sample areas of size less than 10^3 cells. For some combinations, OF-SAR was highly non-linear even when sample areas were around 10^3 cells due to dispersal beyond the isolated habitat fragments (see Figure S8).

Before analyzing the data, we removed simulation runs with parameter combinations resulting in the extinction of all species or when either RAR, SAR or OF-SAR could not be fitted for the data at all. For example, in some extreme cases, all species occurred effectively everywhere, and thus RAR could not be constructed, as no species was endemic to any proper subarea. Finally, to exclude unreasonably well- or poor-performing assemblages due to extreme parameter values, we only considered simulation runs with at least 50 and at most 450 species out of the original 500 species. The final data set constituted of 460 cases out of the initial 840 cases defined by the parameter combinations in Table S1. The statistics for the resulting slopes of RAR, SAR and OF-SAR are given in Table S2.

To analyze the effects of different parameters on the slopes of RAR, SAR and OF-SAR, we used linear regression with each model parameter as an explanatory variable to predict the slope. We used the average values for parameters speciefied by range (colonization rate, extinction rate and dispersal range; see Table S1). The t-values of the linear regression model are given in Table S3.

The slopes reported in the first three rows of Table S2 were obtained by using linear regression on the log-log transformed SAR equation

$$\log \frac{S_{\text{new}}}{S} = z \log \frac{A_{\text{new}}}{A} \tag{17}$$

Table S1: Parameter values in different parameter combinations for computing the RAR, SAR and OF-SAR. Colonization rate and extinction rate indicate the range delimiters for the values. Thus, colonization rates are chosen from ranges $(0, .25]$, $(.25, .5]$, and so on. Dispersal values are similarly chosen from the given sets. The remaining parameters have any of the exact values listed here.

Model parameter	**Value ranges**
Colonization rate (c)	.25, .5, 1.0, 1.5, 2.0
Extinction rate (e)	.025, .05, .1, .15, .2, .25, .3, .4
Dispersal range (α^{-1})	$\{1, \ldots, 4\}$, $\{5, \ldots, 8\}$, $\{9, \ldots, 13\}$
Niche width (γ)	0.1, 0.2
Habitat autocorrelation (ω)	0.5, 1.0, 1.5, 2.0

for SAR and OF-SAR data, and the log-log transformed RAR equation

$$\log \frac{S - S_{\text{loss}}}{S} = z \log \frac{A_{\text{new}}}{A} \tag{18}$$

for RAR data. These slope values were also used for the regression model explaining the effects of different parameters given in Table S3.

For comparison, we also computed the slopes by fitting the data in two alternative ways. The first method consists of using linear regression on the log-log transformed equations $S_{\text{new}} = ca^z$ and $S - S_{\text{loss}} = c(A - a)^z$, where a is the sample area. Secondly, we used non-linear regression on the SAR and RAR equations without log-log transformation and intercept c. These results are summarized in Table S2. All three methods produce similar results for our data. Only the mean slope of OF-SAR has some minor differences.

The effect of dispersal range on OF-SAR We observed that the average dispersal distance of the species affected the scale of the non-linear phase in SAR, and in particular, in OF-SAR when plotted in log-log space. Figure S8 illustrates this phenomenon. The data were generated by running four simulations with the same habitat but different sets of species. In each case, only the distribution of dispersal distances was changed. The simulation was run for 500 time steps on a 256×256 grid with 1000 species with parameters $e \in [0.05, 0.15]$, $c \in [0.5, 1.5]$, $\gamma = 0.1$ and four different ranges of α as given in Figure S8.

Transient times. Figure 3 in the main text was constructed by running a simulation on a 256×256 landscape with no regional stochasticity and 500 species with parameters $c \in [0.5, 1.5]$, $e \in [0.05, 0.15]$, $\alpha^{-1} \in \{1, \ldots, 8\}$ and $\gamma = 0.1$. First, we simulated the system for 1000 time steps and computed RAR, SAR and OF-SAR. Secondly, a part of the habitat was destroyed such that only a single fragment covering 10% of the landscape remained. The simulation was resumed for 1000 time steps. The second step was repeated for 100 times with the reserve positioned randomly each time. Finally, the number of extinctions predicted by RAR, SAR and OF-SAR was compared against the number of extinctions during the simulation.

In this experiment, we used slightly longer simulation times than in the other experiments to ensure that the transient had time to die out. In most cases, the number of

Table S2: Statistics for RAR, SAR and OF-SAR slopes in simulations using the combinations given in Table S1. The table lists the results for three different methods for computing the slopes. The first three rows are from data fitted with linear regression to the log-log transformed SAR and RAR equations with no intercept. These are followed results from fitting the same data to the log-log transformed equation with intercept c using linear regression. Observe that Equations 17 and 18 lack the intercept term and hence the resulting R^2 values in the first three rows may be inflated when compared to the R^2 values given in the subsequent three rows. The final three rows are the results from fitting the data into the power-law equations (Equations 15 and 16) using non-linear regression. In all cases, the same data set with $N = 460$ was used.

	Mean	Median	Standard deviation	R^2 mean	R^2 median
RAR	0.04	0.031	0.033	0.981	0.988
SAR	0.07	0.06	0.049	0.99	0.99
OF-SAR	0.244	0.17	0.22	0.919	0.948
RAR with c	0.041	0.032	0.033	0.893	0.933
SAR with c	0.07	0.06	0.053	0.982	0.986
OF-SAR with c	0.296	0.19	0.28	0.888	0.921
RAR (NLR)	0.04	0.031	0.034	-	-
SAR (NLR)	0.065	0.058	0.048	-	-
OF-SAR (NLR)	0.175	0.147	0.11	-	-

Table S3: The effects of model parameters on the slopes of RAR, SAR and OF-SAR. The table gives the t-value for each explanatory variable (model parameters) in a linear regression model explaining the slope.

	RAR	**SAR**	**OF-SAR**
Colonization rate (c)	-14.45	-16.77	-18.06
Extinction rate (e)	4.636	7.1	13.48
Dispersal range (α^{-1})	-7.23	-10.97	10.46
Niche width (γ)	-7.31	-10.29	-5.96
Habitat autocorrelation (ω)	5.14	19.11	3.84

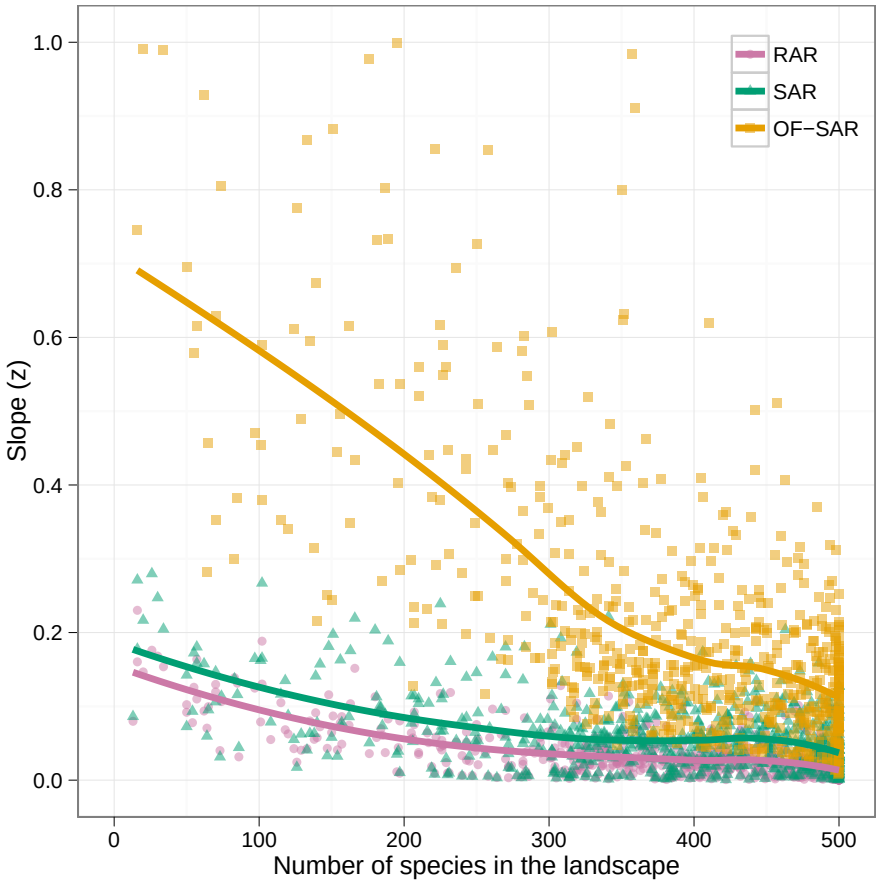

Figure S7: The values of the slopes of RAR, SAR and OF-SAR and against the number of species in quasi-stationary state.

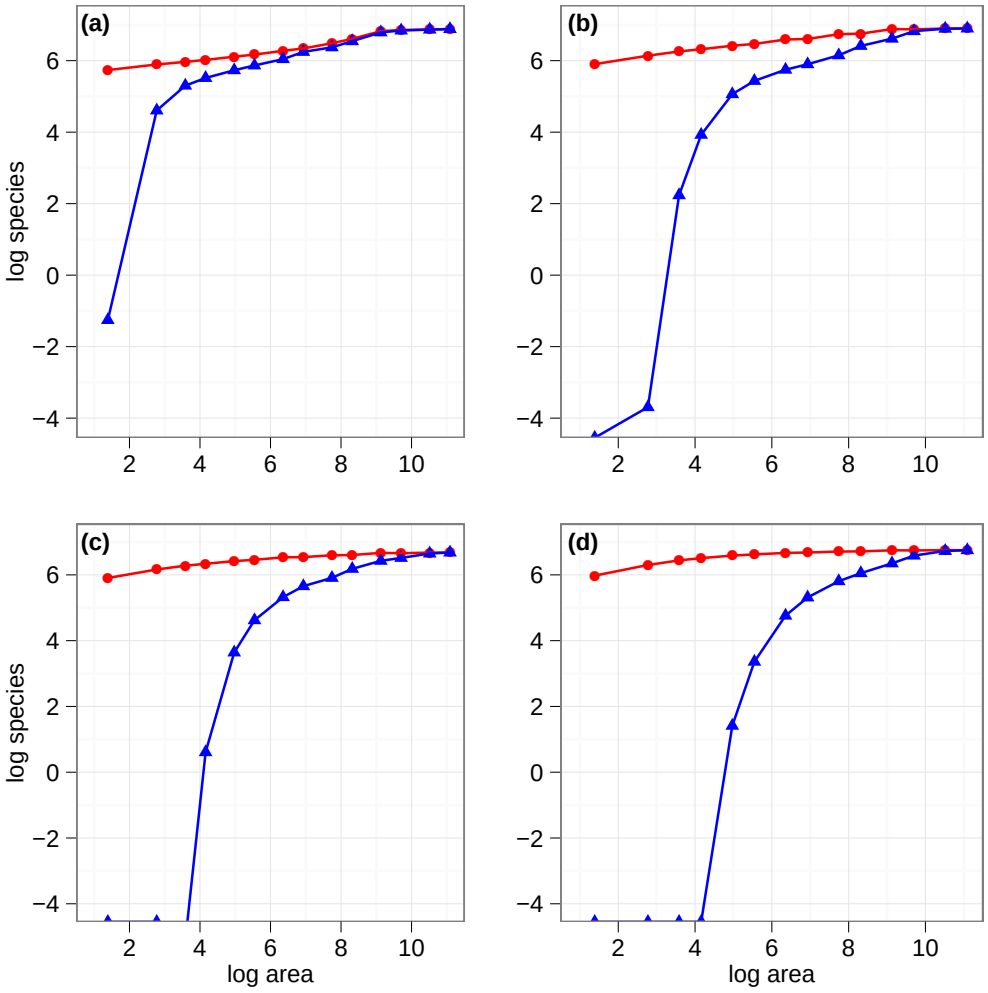

Figure S8: Increasing dispersal distances lengthens the initial non-linear phase of OF-SAR. The average number of species against the sample area is plotted in log-log space. The habitat and the distribution of parameter values remained the same in all plots, except the dispersal distances, which were (a) $\alpha^{-1} \in \{1, 2\}$, (b) $\alpha^{-1} \in \{6, 7\}$, (c) $\alpha^{-1} \in \{11, 12\}$, and (d) $\alpha^{-1} \in \{16, 17\}$. Data points with zero species are shown at the bottom border of the figure.

species decreased dramatically within the first few time steps following habitat loss after which the rate of extinctions gradually slowed down. The length of the transient time varies slightly with the scale of spatial autocorrelation in habitat type: if the habitat had little or no autocorrelation, the transient time is somehwat longer.

The effect of habitat fragmentation. We compared different patterns of habitat fragmentation by running a set of simulations using parameters given in Table S4. We used a landscape of 256×256 cells and applied five different patterns of fragmentation onto the landscape. Before applying habitat loss, the simulation was run for 500 time steps and the state of the system was saved. After destroying habitat, the simulation was resumed for 500 additional time steps. Each fragmentation pattern was repeated 25 times with randomly chosen areas for habitat preservation from the previously saved state. The average number of extinctions was documented. In order to take into account extinctions not caused by habitat loss, 25 reference simulations without any habitat loss were also run for 500 steps. The average number of extinctions that occurred in the reference simulations was subtracted from the average number of extinctions in simulations with habitat loss.

Each pattern destroyed approximately 90% of the habitat but with differences in the spatial structure of the remaining habitat. For the clustered fragmentation patterns, the total number of small fragments was 640, but the distribution of these fragments among clusters varied. The five patterns studied were

- maximal fragmentation with 20 large fragments
- maximal fragmentation with 640 small fragments
- clustered fragmentation with 20% cluster cover and 50% local coverage
- clustered fragmentation with 33% cluster cover and 30% local coverage
- clustered fragmentation with 50% cluster cover and 20% local coverage.

We analyzed the data with a linear regression model. The number of remaining species after habitat loss was explained by the model parameters and the presence of regional stochasticity. The t-values for the explanatory variables are given in Tables S5 and S6. We included the number of extinctions occurring in the case of maximal fragmentation with 640 fragments as an explanatory variable in the clustered fragmentation case.

In order to compare the effects of spatial configuration of habitat, we excluded parameter combinations that yielded assemblages with low species count (less than 300 non-extinct species), as in such cases, the species appeared to be highly intolerant of habitat fragmentation. Figure S9 shows that in most cases with less than 300 species, 90% habitat loss caused the extinction of practically all species.

The comparison in Figure 4 of the main text is based on the following parameters. The size of the landscape was 256×256 and there were initially 250 species. The species parameters were $\alpha^{-1} \in \{4, 5, 6, 7, 8\}$, $c \in [1.5, 2]$, $e \in [0.1, 0.15]$ and $\gamma = 0.1$. For regional stochasticity, the scale of autocorrelation was 1.0 and the parameters of truncated log-normal distribution were $\mu = 0$ and $\sigma = 0.75$ (Figure S2 illustrates this case).

The initial simulation was run for 300 time steps and after habitat loss the simulation was resumed for another 300 rounds. Each pattern was applied (on the same landscape) 25 times and the average number of species remaining was recorded for each pattern type. Figure S10 shows the same data as in Figure 6 of the main text (number of surviving species in the case of clustered fragmentation against maximal fragmentation), but the symbol of the data point indicates whether regional stochasticity was present or absent in the simulation.

Table S4: Parameter values used in the different parameter combinations while analyzing the effects of different fragmentation patterns. The values are listed as in Table S1 with the addition of regional stochasticity parameter. Regional stochasticity can either be absent or present with the range of spatial autocorrelation set to 1 and log-normal distribution with parameters $\mu = 0$ and $\sigma = 0.75$.

Model parameter	**Value ranges**
Colonization rate (c)	.5, 1.0, 1.5, 2.0
Extinction rate (e)	.05, .1, .15, .2, .25
Dispersal range($1/\alpha$)	$\{1,\ldots,4\}$, $\{5,\ldots,8\}$, $\{9,\ldots,13\}$
Niche width (γ)	0.1, 0.2
Habitat autocorrelation (ω)	0.5, 1.0, 1.5, 2.0
Regional stochasticity	enabled, disabled

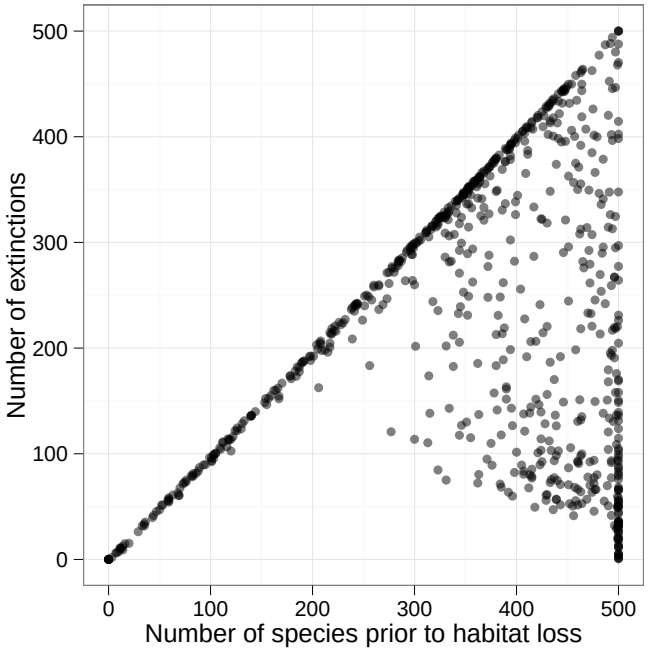

Figure S9: The number of extinctions against the number of species prior to habitat fragmentation. The figure shows the number of extinctions that occurred when the landscape is maximally fragmented with 640 fragments covering 10% of the total landscape area. The datapoints are for the parameter combinations given in Table S4. When the number of species prior to habitat loss is less than 300, most patterns cause the extinction of all species. Hence, to compare different patterns of fragmentation, we disregarded parameter combinations that had <300 species prior to habitat loss.

Table S5: The t-values from regression models where the average number of surviving species in landscapes with 20 and 640 habitat fragments is explained by the spatial autocorrelation of habitat and the species parameters. Only cases where the number of species prior to fragmentation is >300 (out of 500) are included.

	20 fragments	**640 fragments**
Colonization rate (c)	19.17	16.13
Extinction rate (e)	-28.95	-45.97
Dispersal range (α^{-1})	-20.52	-15.03
Niche width (γ)	16.28	9.32
Habitat autocorrelation (ω)	7.68	6.9
Regional stochasticity	-8.29	-10.79
R^2 ($N = 534$)	0.74	0.82

Table S6: The t-values from regression models where the number of surviving species in landscapes with 20 clusters of 32 small fragments (thus a total of 640 fragments) is explained by the number of surviving species in maximally fragmented landscapes (640 fragments randomly located across the landscape) and the model parameters. Only cases where the number of species prior to fragmentation is >300 (out of 500) are included. The table gives the t-values of regression coefficients for three fragmentation patterns in the same initial landscape. The top row gives the cluster cover ratio (c_{C}) and local cover ratio (c_{L}) parameters for the clustered fragmentation pattern. For all cases, 10 % of the landscape area is covered by habitat fragments. All but (*) are significant at $p < 0.001$ level.

Clustered pattern parameters $c_{\mathrm{C}} \cdot c_{\mathrm{L}}$	$0.2 \cdot 0.5$	$0.33 \cdot 0.3$	$0.5 \cdot 0.2$
Species in maximally fragmented case	-1.63 (*)	-12.46	-24.27
Colonization rate (c)	19.86	20.90	20.98
Extinction rate (e)	-19.04	-18.89	-17.70
Dispersal range (α^{-1})	-18.37	-13.64	-12.37
Niche width (γ)	14.16	16.55	19.84
Habitat autocorrelation (ω)	10.13	11.14	10.60
Regional stochasticity	-9.67	-9.53	-8.88
R^2 ($N = 534$)	0.80	0.88	0.93

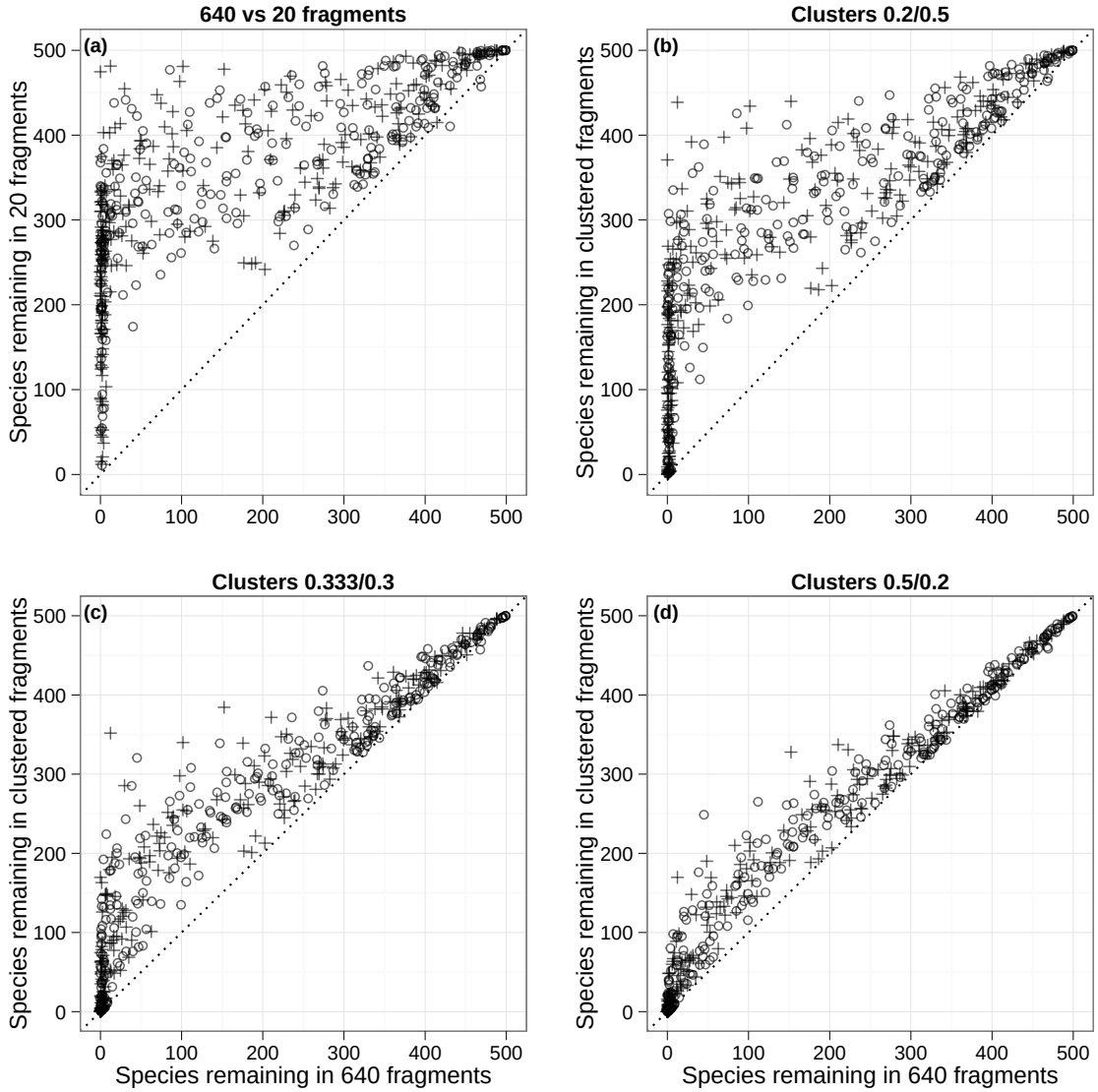

Figure S10: Figure 6 of the main text replotted with the symbol of the data point indicating whether regional stochasticity was present in the simulation or not. Circles (∘) are data points from simulations with no regional stochasticity, whereas points marked with a cross (+) have regional stochasticity.

References

Brewster, C. C. & Allen, J. C. (1997). Spatiotemporal model for studying insect dynamics in large-scale cropping systems. *Environmental Entomology*, 26, 473–482.

Gu, W., Heikkilä, R. & Hanski, I. (2002). Estimating the consequences of habitat fragmentation on extinction risk in dynamic landscapes. *Landscape Ecology*, 17, 699–710.

Ovaskainen, O. & Hanski, I. (2004). Metapopulation dynamics in highly fragmented landscapes. In: *Ecology, Genetics, and Evolution in Metapopulations* (eds. Hanski, I. & Gaggiotti, O. E.). Elsevier Academic Press Amsterdam, pp. 73–104.